arXiv:1506.00531v2 [hep-ph] 18 Jan 2016

Nonperturbative approach to the parton model

Yu.A.Simonov,
Institute of Theoretical and Experimental Physics
117218, Moscow, B.Cheremushkinskaya 25, Russia

January 19, 2016

Abstract

The nonperturbative parton distributions, obtained from the Lorentz contracted wave functions, are analyzed in the formalism of many-particle Fock components and their properties are compared to the standard perturbative distributions. We show that the collinear and IR divergencies specific for perturbative evolution treatment are absent in the nonperturbative version, however for large momenta¡ $\mathbf{p}_i^2 \gg \sigma$ (string tension), the bremsstrahlung kinematics is restored. A preliminary discussion of possible nonperturbative effects in DIS and high energy scattering is given, including in particular a possible role of multihybrid states in creating ridge-type effects.

1 Introduction

The standard partonic model [1, 2, 3, 4, 5] is a basic element of the modern QCD and is widely used in the treatment of high-energy processes, see [6, 7, 8] for a recent review.

The main principle of the standard partonic model is the assumption of the almost free relativistic motion of quarks and gluons with only perturbative interaction mechanism of their evolution, given by the DGLAP equations [9, 10, 11]. In this process, however, as a necessary element occur IR and collinear singularities, which are cured by making appropriate cutoffs, implying that perturbative laws are effective everywhere in the considered region. The neglect of nonperturbative (np) treatment is due to several reasons. First of all, the processes under consideration are in the systems, moving with high velocity, and till recent time one could treat those only in the perturbative manner, using Feynman diagrams for free elementary constituents. Secondly, the study of the behavior of high-excited systems even in the c.m. system in the np approach is not well developed, and the standard np rules here are absent.

An approach, where perturbative and np methods to the processes with high momentum particles were combined, namely the factorization method, is well developed, but needs some corrections [12, 13]. Therefore there is a strong need for the development of the np side of the high energy QCD, using in particular methods available for relativistic np treatment.

During last decades there had been serious efforts in formulating the path integral methods for QCD based on a general dynamics, including perturbative and np contributions [14, 15, 16, 17, 18, 19, 20]. Recently a most advanced version, including also external QED fields, has appeared [21, 22], and the spin-dependent dynamics was treated on the same ground [23].

Basing on this powerful method, the author was able recently to consider the QCD dynamics in the fast moving system, and has discovered, that exploiting the well-known Lorentz contraction effect one immediately obtains the parton scaled distribution from the original np wave function in the c.m. system [24]. In this way the knowledge of the np wave function, or more generally, of the total Fock column of the system in question allows to write down the corresponding parton distribution functions (pdf).

Explicit examples of the unpolarized valence and sea quark and gluon pdf have been given in [25] in comparison with those calculated before in [6, 7, 8] and the similarity of the obtained pdf with the pdf from [6, 7, 8] is striking.

Moreover it was shown in [25], that the polarized pdf of the proton can be obtained from the np proton wave functions calculated in the full three-quark Dirac bispinor formalism (the so-called factorization approach).

The important point stressed in [25], is that pdf can be obtained from the Fock components both in the c.m. and in the fast moving Lorentz frame and the Fock composition coefficients (relative probabilities of components) are boost invariant.

Moreover for the polarized pdf it was suggested in [25] to use the multihybrid model for the excited DIS states, which yields $\frac{1}{2}\langle\Sigma_3\rangle = 0.182$ for $Q^2 = 10$ GeV^2 which is not far from the data (respectively 0.26 for $Q^2 = 3$ GeV^2).

Thus it might be a possible way for the solution of the old proton spin problem [26, 27, 28]. Moreover, the DIS generated polarized pdf are argued to refer not to the ground state proton, but rather to a high excited baryon state with an indefinite spin and large gluon admixture.

In the present paper we write down explicit connection of pdf with Fock components and stress the possibly important role of multihybrid states for pdf of high excited hadrons. We henceforth study the Hamiltonian and wave functions of hybrids and multihybrids and their contribution to pdf's. Finally we turn to the evolution process and make the np analysis of IR and collinear effects, which are finite in the np framework and divergent in the perturbative formalism. We demonstrate how the perturbative picture develops at high momenta, $p \gg \sqrt{\sigma}$, and how it is goes over into the *np* regime at low momenta.

The paper is organized as follows. In section 2 the Fock component structure of pdf is outlined, in section 3 the hybrid and multihybrid states are analyzed and the gluon and quark pdf are calculated in comparison with known data. In section 4 the IR and collinear effects are studied both in the perturbative and np language. Section 5 contains summary and discussion.

Two appendices contain details of derivation. In appendix 1 the path-integral calculation of the standard IR and collinear amplitudes demonstrates the absence of divergencies in the np dynamics. The appendix 2 contains calculation of the triangle and quadratic Feynman diagrams with confinement, which shows how perturbative dynamics occurs for large momenta, $p^2 \gg \sigma$.

2 Parton distributions from Fock components

We follow here the formalism introduced in [25, 31, 32] and write the total Hamiltonian and the Fock wave function as follows

$$\hat{H} = \left(\begin{array}{lll} H_{11}, & V_{12}, & ... \\ V_{21}, & H_{22}, & ... \\ ... & ... & ... \end{array} \right); \quad \hat{H}\Psi_N = (\hat{H}^{(0)} + \hat{V})\Psi_N, \tag{1}$$

where Ψ_N is decomposed in Fock components as follows

$$\Psi_N = \sum_{m\{k\}} c^N_{m\{k\}} \psi_{m\{k\}}, \quad \psi_n(P, \xi, k) \equiv \psi_{n,\{k\}} \tag{2}$$

Here $m\{k\}, \xi$ refer to the number and types of constitients $(q, \bar{q}, g)$, modes of excitations, spin and momentum projections etc.

The orthogonality conditions look like

$$\int \Psi^+_N \Psi_M d\Gamma = \sum_{m\{k\}} c^N_{m\{k\}} c^M_{m\{k\}} = \delta_{NM}. \tag{3}$$

$$\int \psi^+_{m\{k\}} \psi_{n\{p\}} d\Gamma = \delta_{mn} \delta_{\{k\}\{p\}}. \tag{4}$$

From (1) one finds the equation for $c^N_{m\{k\}}$

$$c^N_{n\{p\}} (E_N - E^{(0)}_{n\{p\}}) = \sum_{m\{k\}} c^N_{m\{k\}} V_{n\{p\},m\{k\}} \tag{5}$$

where

$$V_{n\{p\},m\{k\}} = \int \psi^+_{n\{p\}} \hat{V} \psi_{m\{k\}} d\Gamma. \tag{6}$$

The Fock component approach was exploited earlier in [29], see [30] for more references, in the framework of the light-cone formalism and perturbative dynamics for the polarized parton distributions. Below we shall handle the np components in the unpolarized case, and in the next section specifically for the multihybrid states.

In what follows we shall have in mind the large N_c limit, classifying different contributions to Ψ_n, namely in the leading order all states are made of gluons only (glueballs) or of hybrids: $q, \bar{q}$ plus any number of gluons. In the next order of the $1/N_c$ expansion the decay into two bound states due to the process $g \to q\bar{q}$ is possible.

We are using the following normalization condition as in [25] for the n particle bound state.

$$\int |\tilde{\varphi}_n(\mathbf{k}^{(1)}, \mathbf{k}^{(2)}, ...\mathbf{k}^{(n)}|^2 \prod_i \frac{d^3\mathbf{k}^{(i)}}{(2\pi)^3} (2\pi)^3 \delta^{(2)}(\sum_i \mathbf{k}^{(i)}_\perp) \delta(1 - \sum_i x_i) = 1 \tag{7}$$

and $dk^{(i)}_\parallel = M_0 dx_i$, where M_0 is the c.m. energy (mass) of system. Writing (7) as $\int |\tilde{\varphi}_n|^2 d\tau_n = 1$, one can write the u, d, and g distributions trough the Fock components $\tilde{\varphi}_{3q}, \tilde{\varphi}_{4q\bar{q}}, \tilde{\varphi}_{3qg}$, as follows ($4q\bar{q} = uuud\bar{u}$)

$$u(x, k^2_\perp) = \sum_{n=3q,4q\bar{q}} u_n(x, k^2_\perp) = |c_{3q}|^2 \int |\tilde{\varphi}_{3q}|^2 d\tau_{3q} \sum_{i=1,2} \delta^{(2)}(\mathbf{k}^{(i)}_\perp - \mathbf{k}_\perp) \delta(x_1 - x) +$$

$$+ |c_{4q}|^2 \int |\tilde{\varphi}_{4q\bar{q}}|^2 d\tau_{4q\bar{q}} [\sum_{i=1}^{3} \delta^{(2)}(\mathbf{k}^{(i)}_\perp - \mathbf{k}_\perp) \delta(x_i - x) + \tag{8}$$

$$+|c_{3qg}|^2\int|\tilde{\varphi}_{3qg}|^2\sum_{i=1,2}^{3}\delta^{(2)}(\mathbf{k}_\perp^{(i)}-\mathbf{k}_\perp)\delta(x_i-x)+...,$$

$$\bar{u}(x,k_\perp^2)=\int|\tilde{\varphi}_{4q\bar{q}}|^2 d\tau_{4q\bar{q}}\delta^{(2)}(\mathbf{k}_\perp^{(5)}-\mathbf{k}_\perp)\delta(x_5-x)+..., \tag{9}$$

$$g(x,k_\perp^2)==\int|\tilde{\varphi}_{3qg}|^2\delta\tau_{3qg}\delta^{(2)}(\mathbf{k}_\perp^{(4)}-\mathbf{k}_\perp)\delta(x_4-x)+.... \tag{10}$$

Assuming equal contributions of additional q and $\bar{q}$, one can write the standard relations

$$u^v(x,k_\perp^2)=u(x,k_\perp^2)-\bar{u}(x,k_\perp^2) \tag{11}$$

$$\int u^v(x,k_\perp^2)d^2\mathbf{k}_\perp dx=2(|c_{3q}|^2+|c_{4q\bar{q}}|^2+|c_{3qg}|^2+...)=2, \tag{12}$$

where we have used the total orthonormality condition (3), a similar relation for the d quark, $d^v(x,k_\perp^2)$ obtains from (8), (9), replacing the sums $\sum_{i=1,2}$ and $\sum_{i=1}^3$ by the terms with $i=3$ and $i=4$ respectively, resulting in the normalization equation

$$\int d^v(x,k_\perp^2)d^2\mathbf{k}_\perp dx=|c_{3q}|^2+|c_{4q\bar{q}}|^2+|c_{3qg}|^2+....=1 \tag{13}$$

From (12), (13) one easily obtains the Gross-Llevellin-Smith and Adler relations for u^v and d^v.

We now turn to the momentum relations, and to this end we make evident the x dependence of each pdf, namely, as shown in [25], Eqs. (17), (18), the dependence of $\tilde{\varphi}$ on $p_\perp^{(i)}, x_i$ enters in the form, where there are present the c.m. values of the i-th longitudinal momentum $p_{\parallel i}^{(0)}$ and the c.m. energy of the i-th quark, antiquark or gluon, namely

$$x_i=\frac{p_{\parallel i}}{P}=\frac{p_{\parallel i}^{(0)}+v\varepsilon_i^{(0)}}{P\sqrt{1-v^2}},\quad P\sqrt{1-v^2}=M_0 \tag{14}$$

or

$$p_{\parallel i}^{(0)}=M_0\left(x_i-\frac{\varepsilon_i^{(0)}}{M_0}\right),\ v\to 1 \tag{15}$$

and writing in $\tilde{\varphi}$ only momenta of the i-th particle, one has

$$\tilde{\varphi}(\mathbf{p}_{\perp i}^{(0)},p_{\parallel i}^{(0)})=\tilde{\varphi}(\mathbf{p}_{\perp i}^{(0)},M_0(x_i-\nu_i)), \tag{16}$$

where $\nu_i = \frac{\varepsilon_i^{(0)}}{M_0}$ is a part of the total mass contributed by the i-th c.m. energy. The $|\tilde{\varphi}|^2$ depends on x_i in the contribution $(\mathbf{p}_{\perp i}^{(0)})^2 + (M_0(x_i - \nu_i))^2 = \mathbf{p}_i^2$.

The parton distribution in the hadron is expressed via the np boundstate wave function φ_N as

$$D_h^q(x, k_\perp) = \sum_N |c^N|^2 \prod_{r=1}^{N} \frac{d^2\mathbf{k}_{\perp r} dx_r}{(2\pi)^3} \delta^{(2)} \left(\sum \mathbf{k}_\perp\right) \delta \left(1 - \sum_1^N x_r\right) \times$$

$$\times M_0^N |\tilde{\varphi}_N|^2 \sum_j \delta^{(2)}(\mathbf{k}_\perp - \mathbf{k}_{\perp j}) \delta(x - x_j) \tag{17}$$

and it satisfies the normalization conditions

$$\int d^2 k_\perp dx D_H^q(x, k_\perp) = N_h^j \tag{18}$$

$$\int d^2 k_\perp x dx D_H^q(x, k_\perp) = 1. \tag{19}$$

Taking into account (12), (13), (19), one can write for the proton pdf's the normalization condition

$$\int_0^1 dxx[u(x) + d(x) + \bar{u}(x) + \bar{d}(x) + g(x)] = 1. \tag{20}$$

We now turn to the np description of the Fock components $\tilde{\varphi}_N(\mathbf{k}_{1,\dots}\mathbf{k}_n)$.

3 Multihybrid Fock components of a hadron

It is clear, that the general equation (5) for the Fock components

$$c_{n\{p\}}^N (E_N - E_{n\{p\}}^{(0)}) = \sum_{m\{k\}} c_{m\{k\}}^N V_{n\{p\},m\{k\}} \tag{21}$$

contains different stages of evolution $n\{p\}$, each of these is the one or more bound states of $q, \bar{q}$ and g, i.e. of mesons, baryons, glueballs, and hybrids. In the lowest order of the expansion in $1/N_c$, initial (primordial) mesons and baryons are connected only to mesohybrids and baryohybrids respectively, containing arbitrary number of gluons. In the next order of $1/N_c$ one of the gluons can create the $q\bar{q}$ pair and split the total bound state into hadrons

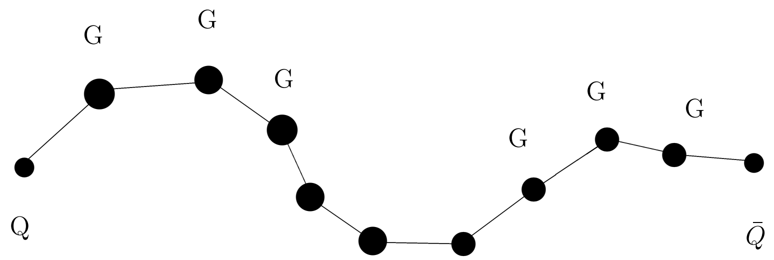

Figure 1: The multihybrid meson configuration with n gluons inside a confining string

etc. Therefore it is of interest to study the spectrum and wave functions of multihybrids and we shall do it for a mesonic multihybrid, see [33, 34, 35, 36] for earlier discussion of one-gluon hybrids, [37, 38, 39, 40, 41, 49, 50] for the theory of hybrids in the field-correlator formalism, [44, 45, 46, 47, 48, **?**, **?**, 51, 52, 53] for the treatment in the framework of potential and QCD sum rule methods, [54, 55] for lattice data, and [56] for a review.

We consider as in [31, 32] (Fig. 1) the system of n gluons on the string, connecting quark ($i=1$) and antiquark ($i=n+2$) and we are using as it is usual for the path-integral Hamiltonian method [21, 22, 23], the einbein form, with effective masses ω_a, ω_b for $q\bar{q}$ and $\omega_i, i=1,...\,n$ for gluons and ν_k- parameters, replacing the linear confinement pieces between $q, g, ..., \bar{q}, \quad \sigma|\mathbf{r}_k|, \quad k = 1,...\,n+1$, by the quadratic terms $\sigma|\mathbf{r}_k| \approx \frac{1}{2}\left(\nu_k + \frac{\sigma^2\mathbf{r}_k^2}{\nu_k}\right)$, and ν_k to be found from the stationary point analysis of the total energy – this procedure is known to yield accuracy of the order $5 \div 10\%$.

The total Hamiltonian (without gluon exchange and spin-dependent terms) is

$$H(\mathbf{P}) = \sum_{i=a,b} \frac{\mathbf{p}_i^2 + m_i^2}{2\omega_i} + \frac{a}{2} + \frac{\mathbf{P}^2}{2a} + \frac{\sigma^2}{2}\sum_{k=1}^{n+1}\frac{\mathbf{r}_k^2}{\nu_k} + \sum_{i=1}^{n}\frac{\mathbf{p}_i^2}{2\omega_i} \tag{22}$$

where $a = \sum_{i=1}^{n+2}\omega_i + \sum_{k=1}^{n+1}\nu_i$, and ω_i, ν_i are to be found from the stationary point conditions

$$\frac{\partial H}{\partial \omega_i} = \frac{\partial H}{\partial \nu_i} = 0 \rightarrow \frac{\partial E(\mathbf{P})}{\partial \omega_i} = \frac{\partial E(\mathbf{P})}{\partial \nu_i} = 0. \tag{23}$$

It is easy to see, that using the l.h.s. of (23) one arrives at the "relativistic model of hybrids" in the sense of Godfry and Isgur [57], we shall instead use the r.h.s. form, which will give us a simple result for $E(\mathbf{P})$ and wave functions (the "einbein method").

We start with the c.m. system, $\mathbf{P} = 0$, and introduce a trial wave function

$$\Psi_0 = N\exp\left[-\sum_{k=1}^{n+1} \alpha_k \mathbf{r}_k^2\right], \quad N = \prod_{k=1}^{n+1} \left(\frac{\pi}{2\alpha_k}\right)^{-3/4}. \tag{24}$$

Leaving details of the calculation to the appendix 1, we write below the result of the minimization (denoted with the superscript (0)) with respect to $\{\nu_k, \omega_i, \alpha_k\}$ in the limit $m_a = m_b = 0,\ n \to \infty$

$$\omega_i^{(0)} = \nu_i^{(0)} = \left(\frac{3\sqrt{2}}{2}\sigma\right)^{1/2} \approx 0.62\ \text{GeV}\ \equiv \omega_0, \quad \alpha_i^{(0)} = \frac{\sigma}{2\sqrt{2}} \tag{25}$$

$$M^{(n)}_{\min(\alpha,\nu,\omega)} = 2\omega_0 n + O(1/n) \cong 1.24\ n\ \text{GeV}. \tag{26}$$

The average intergluon distance is found to be

$$\mathbf{r}_0 \equiv \sqrt{\langle \mathbf{r}_k^2 \rangle} = \sqrt{\frac{3}{\sqrt{2}\sigma}} = 0.68\ \text{fm}. \tag{27}$$

The value (26) is an upper limit, and the actual mass should be lower. To check the accuracy of our calculations we consider the case of the simplest hybrid state: $q\bar{q}g$, in which case the same type of the trial wave function yields $M^{(1)} \cong 2.1$ GeV, while more accurate calculations [37] give the lowest mass $M^{(1)} \approx 1.54$ GeV.

Hence one can conclude, that the energy interval between the states of n and $(n+1)$ hybrids (one additional gluon) is

$$\Delta M = M^{(n+1)} - M^{(n)} \approx 0.8 \div 1\ \text{GeV}. \tag{28}$$

The energy intervals of the transverse vibrational modes $\Delta E^{(TVM)}$ and longitudinal vibrational modes $\Delta E^{(LVM)}$ have been calculated in [37] last reference, for the case of the gluon string with fixed ends and are equal

$$\Delta E^{(LVM)} = \frac{0.53\ \text{GeV}}{[R\ (\text{fm})]^{1/3}}, \quad \Delta E^{(TVM)} = \frac{0.69\ \text{GeV}}{R\ (\text{fm})}. \tag{29}$$

From (29) one can conclude, that the lowest types of excitations for long multigluon strings are of the TVM and LVN types, while spin-spin interaction interval ΔM_{ss} is of the order of 0.3 GeV. It is understandable, that for large n there appear collective excitations of the TVM and LVM types.

We now turn to the partonic form of our n-gluon hybrid wave function, from (24) one has in the k-space

$$\tilde{\varphi}_N^2(\mathbf{k}_1, ...\mathbf{k}_{N-1}) = \frac{1}{M_0}\left(\frac{2\pi}{\alpha}\right)^{\frac{3}{2}(N-1)} \exp\left(-\sum_{i=1}^{N}\frac{\mathbf{k}_i^2}{2\alpha}\right), \quad N = n+2. \tag{30}$$

Here $\tilde{\varphi}_n$ is normalized as in(7), M_0 is the total energy in the c.m. system.

From (30) one can deduce that the wave function for the i-th degree of freedom in (30) can be written in the form of (16) $\tilde{\varphi}^2(\mathbf{k}_i^2) = \tilde{\varphi}^2(\mathbf{k}_\perp^2 + M_N^2(x_i - \nu_i)^2)$ and inserted in (17) to produce the pdf of the multihybrid state. Integrating over $d\mathbf{k}_{\perp i}\, dx_i$ in (17) one finally obtains with the notations $\kappa^2 = 2\alpha, M_0 \to M_N$ the form of pdf suggested and studied in [25]

$$f_i^{(N)}(M_N|x-\nu|) = \xi_i^{(N)}\frac{M_N}{\kappa}\exp\left(-\frac{M_N^2}{\kappa^2}(x-\nu_i)^2\right) \tag{31}$$

where $i = g, q; \xi_i^{(N)}$ is defined by normalization condition

$$\int_0^1 f_i^{(N)}(x)dx = 1 \tag{32}$$

and we have introduced effective masses of quarks and gluons $M_N = 3\omega + Nm$, $3\omega = M_p$, so that

$$\nu_g = \frac{m}{M_N}, \quad \nu_q = \frac{\omega}{M_N}. \tag{33}$$

Using (31) one can proceed as in [25] to calculate the pdf's of gluons $g(x)$ and valence u quarks $u(x)$, and we shall neglect as in [25] the contribution of the nucleon itself, so that in multihybrids $N \geq 1$, and concentrate on the region of small x, $x \lesssim 0.1$. One has for a sequence of N- multihybrids with with probabilities $|C_N|^2$

$$u_v(x) = 2\sum_{N=1}|C_N|^2\xi_q^{(N)}\frac{(M_p + m_N)}{\kappa}\exp\left(-\frac{M_N^2}{\kappa^2}(x-\nu_q)^2\right) \tag{34}$$

$$g_v(x) = \sum_{N=1}^{\infty}|C_N|^2\xi_g^{(N)}N\frac{M_p + N_m}{\kappa}\exp\left(-\frac{M_N^2}{\kappa^2}(x-\nu_g)^2\right). \tag{35}$$

In what follows we shall slightly generalize the discussion in [25] and assume that $|C_N|^2$ decrease as $N^{-\gamma}, 1 < \gamma < 2$,

$$\sum |C_N|^2 = 1, \quad |C_N|^2 = N^{-\gamma} |\bar{c}|^2, \quad |\bar{c}|^2 = \zeta(\gamma), \tag{36}$$

where $\zeta(\gamma)$ is the Riemann dzeta-function, $\zeta\left(\frac{3}{2}\right) = (2,62)^{-1}$.

As a result one obtains for $g(x)$ and $u(x)$

$$g(x) = |\bar{c}|^2 (a_1 x^{\gamma-2} + a_2 x^{\gamma-3}), \tag{37}$$

$$u_n(x) = |\bar{c}|^2 (b_1 x^{\gamma-1} + b_2 x^{\gamma-2} + b_0), \tag{38}$$

where a_i, b_i depend on parameters $\kappa, m(\omega = \frac{M_p}{3} = 0.31(\text{GeV})$. We can fix these parameters, as in [25], using the explicit form of the lowest hybrid with $N = 1$ from [33, 37], $\kappa = \frac{m}{2} = 0.313$ GeV.

In this way we have the only fitting parameter γ, which we can choose to correspond roughly to the gluon pdf at $Q^2 = (3 \div 10)$ GeV^2. In this way we can consider $g(x)$ and $u(x)$ as starting pdf in the DGLAP evolution equations instead of standard initial state functions with roughly 15-20 free parameters. Following [25] we take $\gamma = 3/2$ and obtain

$$a_1 = 1.5, \quad a_2 = 1, \quad b_1 = 2.82, b_2 = 2.70. \tag{39}$$

As a result one obtains $xg(x)$ at the points $x = 10^{-2}; 10^{-1}$ to be equal to 3.87; 1.38, which is close to the PDG data at $Q^2 = 10$ GeV^2, respectively 5; 1.5 (cf. Fig 19.4 in the last ref. of [6, 7, 8]).

The same type of similarity between (38) and and PDG data exists for $xu_v(x)$, which implies, that the sequence of multihybrid states can be used as a part of evolution process. It is also interesting that $g(x)$ contains an additional power of x^{-1} as compared to $u_v(x)$, which also nicely corresponds to the data. One can now check whether multihybrids can produce reasonable amount of sea quark pdf. This check was done in [25], where it was shown that the $q\bar{q}$ DGLAP evolution of (37) in the interval (1-10) GeV^2 produces $\bar{u}(x, 10\ \text{GeV}^2) \approx 0.04 g(x, 10\ \text{GeV}^2)$, in good agreement with PDG data [6].

As a final check we compute $g(x, Q^2 = 10^4\ \text{GeV}^2)$, as a result of the DGLAP evolution of our form (37), (39) for $Q^2 = 10$ GeV^2 and obtain

$$\frac{dg}{d \ln Q^2} = \frac{3\alpha_s}{\pi} \varphi(x), \varphi(x) \simeq |\bar{c}|^2 (0.917 x^{-3/2} + x^{-1} - 3.4 x^{-1/2}) \tag{40}$$

which yields roughly $xg(x = 0.01, 10^4\ \mathrm{GeV}^2) \approx 3.5$, whereas the PDG data gives a 2.5 larger value. This might point out to an additional mechanism (e.g. of the BFKL type) at very large Q^2 and small x.

We have considered above only the region of small x, $x < 0.1$. Larger x need some modifications. Namely, introducing the quark-counting rule factor $(1-x)^{\rho(N)}$ into (34), (35), where $\rho(N)$ is growing with N, one obtains modified normalization factors $\xi_i^{(N)}$ and an effective upper limit in the summation over N, $N_{\max} \sim \frac{Q}{m}\sqrt{1-x}$, since $M_N^2(eff) \sim s$. These replacements do not essentially change our results for $N_{\max} \gg 1$, but are essential for very small x, where the contribution of the multihybrid contribution is strongly damped by $\rho(N)$ as compared to the nongluonic excited nucleon states.

Concluding this section, we have shown that the multihybrid mechanism at the initial or intermediate stage of parton evolution can be considered on the same ground as other realistic contributions and may have its own part in the final reaction products.

Note, that our small x asymptotics, $u_g(x) \sim x^{-\gamma}$, is different from the reggeon-type asymptotics, and is a result of the multihybrid state formation in the general multigluon ladder-type diagrams. It is possible, that the latter provide both types of asymptotics, the more common "hard" momentum distribution when each loop in the ladder with a large rapidity ratio yields $\left(\alpha \ln \frac{1}{x}\right)$, and a soft (or coherent) momentum distribution, as in (30), which possibly occurs for very large s. We study below in the next sections and appendix these two regimes in the example of the square box diagram with confinement, and discover two possible regimes, depending on whether the external momenta are much larger, or comparable with the string tension.

Significantly as one of possible signals one can consider the ridge-type configurations [72, 73, 74], where experimental signals are along a straight line, which mimicks the average form of a large multihybrid with $N \gg 1$.

4 Nonperturbative vs perturbative regimes

The purpose of the present section (and the Appendix 2) is to demonstrate, that IR and collinear singularities are absent in QCD (in contrast to QED), which however does not imply the absence of the logarithmic and double logarithmic terms in the perturbative series.

As a standard approach to the evolution and cross sections in high-energy QCD one is using the QED processes of $e \to e'\gamma$, $\gamma \to e^+e^-$ with the IR and collinear singularities and perform the analogous perturbative procedure in QCD, leading to the singularities e.g. in fragmentation functions and average number of partons etc. However, in QCD both IR and collinear singularities are absent, as we demonstrate below, and the multiplicative gluon emission leads to the formation of heavy multihybrid states, in contrast to the QED, where the multiphoton emission is a real background process, which is treated introducing an experimental bound – the minimal energy E_l of the registered photons [58, 59, 60].

As a consequence in QED the observed cross section of the high q^2 process contains Sudakov double-logarithmic corrections of the type $\frac{\alpha}{\pi}\ln\left(\frac{q^2}{m^2}\right)\ln\left(\frac{q^2}{E_l^2}\right)$.

In QCD the minimal energy E_l is absent, since gluons are never emitted as free particles and its emission inside hybrid states costs an increase in the total mass of ground states $\Delta E \approx O(1\text{ GeV})$. Moreover, the quark mass m_q cannot enter in the final equations due to confinement for $m_q < \sqrt{\sigma} = 0.42$ GeV, hence the multigluon emission might have another structure. In the DGLAP evolution equations this difficulty is avoided considering evolution of quark, antiquark and gluon pdf's $f_f(x, Q)$ as functions of momentum scale Q, with the kernels ensuring logarithmic dependence on Q^2 (a weak violation of the Bjorken scaling), and on x at small x.

As we argue below in this section, and in the Appendix 2, in QCD the IR and collinear singularities are absent, but the perturbative series terms can indeed have the known logarithmic form, and the role of the cut-off parameter is played by the string tension, so that at high momenta, $p^2 \gg \sigma$, the perturbative kinematics prevails.

We start with the standard perturbative picture. To put the problem in the most simple form, consider the process $e^+e^- \to q\bar{q}g$, with the cross section for free $q, \bar{q}, g$ equal to (see e.g. [5], chapter 17)

$$\frac{d\sigma}{dx_1 dx_2}(e^+e^- \to q\bar{q}g) = \sigma_0 \left(3\sum_f Q_f^2\right) \frac{2\alpha_s}{3\pi} \frac{x_1^2 + x_2^2}{(1-x_1)(1-x_2)} \tag{41}$$

where x_1, x_2, x_3 are ratios of $q, \bar{q}$ and g energies to the e^+e^- energy $\sqrt{s}$ and one can write

$$1 - x_1 = x_2 \frac{E_g}{\sqrt{s}}(1 - \cos\theta_{2g}), \quad 1 - x_2 = x_1 \frac{E_g}{\sqrt{s}}(1 - \cos\theta_{1g}), \tag{42}$$

and these denominators arising from the virtual propagators of quarks: $(p_1')^2 - m_1^2 = (p_1 + p_g)^2 = m_1^2 + \sqrt{s}E_g x_1(1 - \cos_{1g})$. One can see the collinear

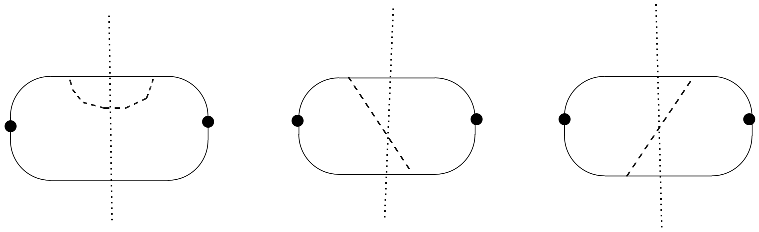

Figure 2: The Feynman diagrams for the $q\bar{q}$ Green's function, which contribute to the $q\bar{q}g$ cross production cross section

and IR singularities of the unconfined QCD, which are essential element in the balance of the integrals defining the terms of the perturbative series.

In general, the bremsstrahlung probability can be written as

$$dP_{brems} = \frac{\alpha C_N}{\pi^2} \frac{d^2 k_\perp}{k_\perp^2} \frac{dx}{x}, \tag{43}$$

where $x \sim \frac{m^2}{s}$, or else $x \sim \frac{Q^2}{s}$ for the deep inelastic evolution. In the series of the gluon cascade amplitude (the Regge-Gribov amplitude) one has for the term with n internal lines

$$I_n \sim (c\alpha_s)^n \int_x^1 \frac{dx_n}{x_n} \int_{x_n}^1 \frac{dx_{n-1}}{x_{n-1}} ... \int_{x_2}^1 \frac{dx_1}{x_1} \approx \frac{1}{n!} (c\alpha_s \ln \frac{1}{x})^n \tag{44}$$

which yields for the total sum the standard answer

$$\sum_n I_n \sim \exp{(c\alpha_s \ln \frac{1}{x})} \sim \left(\frac{s}{m^2} \right)^{c\alpha_s}. \tag{45}$$

One can see, that the crucial property of the Regge-type behavior (45) is the bremsstrahlung-type energy distribution $\frac{dx}{x}$, at each step of the gluon cascade, as it is also in (41). Therefore it is interesting to calculate the same cross section (41) with confinement taken into account.

To make a comparison with the *np* (confined) QCD, one must calculate the diagrams, shown in Fig.2, and one has in mind, that all the area inside the outer contour of the diagrams, is covered with the confining film (shown by the vertical lines in Fig. 3).

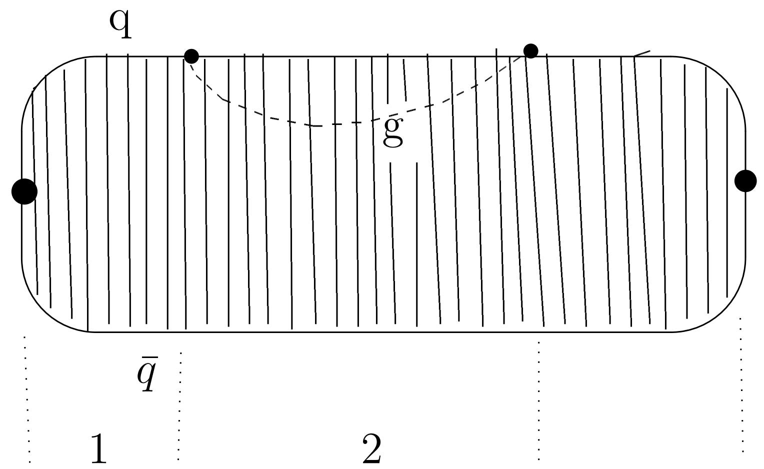

Figure 3: The path integral representation of the $q\bar{q}$ Green's function. The regions denoted by 1,2,3 refer to $q\bar{q}, q\bar{q}g$ and $q\bar{q}$ intermediate states respectively

We calculate the $q\bar{q}$ Green's function in the path integral formalism incorporating confinement and gluon exchange in appendix 1 and write down the result in the form, appropriate for the Fock component language, namely

$$G_{q\bar{q}}(E) = \frac{\langle Y\rangle}{(2\omega)^2}\varphi(0)\frac{1}{E-E_1}\frac{V_{12}}{\sqrt{2\omega_g}}\frac{1}{E-E_2}\frac{V_{23}}{\sqrt{2\omega_g}}\frac{1}{E-E_3}\varphi(0) \tag{46}$$

where the gluon creation matrix elements V_{ik} are expressed via overlap matrix elements of meson and hybrid wave functions [31, 32, 61, 62], and ω, ω_g are average energies (from the Hamiltonian minimization) of quarks and gluon.

From [32] one has

$$\frac{V_{12}}{\sqrt{2\omega_g}} = \frac{V_{23}}{\sqrt{2\omega_g}} \cong g \cdot 0.08\text{GeV} \tag{47}$$

To obtain the cross section $e^+e^- \to hybrid(q\bar{q}g)$, one takes the discontinuity of (46) in energy due to the factor $\frac{1}{E-E_2}$ and obtains

$$d\sigma(e^+e^- \to hybrid) \sim \left[\varphi(0)\frac{V}{\sqrt{2\omega g}}\frac{1}{E_2-E_1}\right]^2 \delta(E-E_2) \tag{48}$$

where $E_2 - E_1 \approx 0.8 \div 1$ GeV for $E_1 \approx m_\rho$, $E_2 = M_{hybrid}$ and one does not have any IR or collinear singularities in agreement with our discussion and the beginning of this section. It is also essential, that the structure of the final states in (48) in the np regime is quite different from the perturbative QCD, namely for low energy resolution one should sum up over all collective states of the hybrid, and in the case of high energy and multihybrid state the overall entropy of states can be very large.

To resolve the apparent contradiction one can consider the Feynman diagrams, shown in Figs. 4, 5, where we take into account confinement as the area law of the Wilson loop, e.g. formed by the 4 sides of the rectangular in Fig. 5.

$$W(C) = \exp(-\sigma S_{min}(1,2,3,4)) \tag{49}$$

As shown in the appendix 2, the approximate answer for this diagram is

$$G_4(p_i) = \prod_{i=1}^{4} \int d^4 q_i \int_0^\infty ds_i e^{-s_i(m_i^2+q_i^2)} J_\sigma(s_i, b^{(i)}) \tag{50}$$

and

$$b^{(i)} = p_i - q_i + q_k \tag{51}$$

where q_1, q_k are momenta on the adjacent lines in the vertex i. The property of J_σ is such, that at large $p_i, q_k, (b^{(i)})^2 \gg \sigma$, it becomes a product of the vertex δ- functions

$$J_\sigma((b^{(i)})^2 \gg \sigma) \sim \prod_{i=1}^{4} \delta^{(4)}(b^{(i)}) \tag{52}$$

As a result $G_4(p_i)$ coincides in this limit with the standard perturbative answer, where the bremsstrahlung property (43) appears, but now for large (as compared with $\sqrt{\sigma}$) momenta.

At the same time for low momenta, $(b^{(i)})^2 \lesssim \sigma$, one has four d^4q integrations, which exclude any possibility of IR or collinear singularities.

Thus one may imagine for a sequence of ladder-type diagrams two types of asymptotics, depending on the internal momenta distributions: a) (47), (48) for perturbatively ordered momenta; b)multihybrid-type asymptotics considered in the previous section for np ordered momenta, $|\Delta P_i| \sim \sqrt{\sigma}$.

We are now coming to a possible general picture of np evolution in DIS or high energy hadron reactions. We assume, that in the intermediate or initial state there appears a multihybrid state (or a family of multihybrid states with close-by masses). This multihybrid state originally (by evolution) is perturbatively (bremsstrahlung-type) ordered, which corresponds to the reggeon-like asymptotics and the BFKL-type desctiption, but has a possibility to develop into a quark stable multihybrid state, described in the previous section. It subsequently decays into more multihybrids and finally into $q\bar{q}$ and $3q$ hadrons, due to perturbative and np string breaking. In this way the gluons contribute the most amount of the collision energy at this primordial stage, which in the evolution process is transferred to the final hadrons.

5 Summary and discussion

We have tried above to formulate main features of the np approach to the high energy production of hadrons in DIS or hadron-hadron collisions, which might be an alternative or a complement to the standard QCD picture [6, 7, 8]. The basis of our approach is the fact, that the Lorentz contraction rule of wave functions automatically leads to the parton-like form of its momentum depenence [24], and one the c.m. wave function to rewrite it in terms of partonic variables, $\mathbf{p}_\perp$ and x, namely $\mathbf{p}^2 = \mathbf{p}_\perp^2 + M_0^2(x-\nu)^2$, where M_0 is the c.m. energy of the object.

This allows to write down the pdf's of the object, e.g. of the fast proton in terms of the c.m. wave function, as it was done in [25] both in the polarized and unpolarized cases. In this way one obtains the np components of the partonic set of pdf's, and the point is how to represent wave function of the arbitrary moving complex object and subsequently how to extract from it the total set of pdf's: valence and sea for any quark flavor.

This is done at the beginning of the present paper with the help of Fock components of the Fock column wave function, where each line corresponds to a definite ensemble of $q, \bar{q}, g$ with the same total quantum numbers. We have expressed pdf's as a sum over Fock components, satisfying usual normalization conditions. We have also shown before in [25], that the normalization of the Fock components is boost invariant, and hence it is possible and often convenient to calculate pdf's from the Fock column in the rest frame.

Using that, we have considered in section 3 the basic building block of the high excited Fock column – the multihybrid state, which may be one of the basic primordial state of the high energy evolution of the Fock column in the $1/N_c$ expansion, where the $g \to q\bar{q}$ decays are $O(1/N_c)$, as compared to gluon creation and absorption.

We have found the wave function of the multihybrid and discovered that it is highly correlated with an average energy per quark and gluon around 0.6 GeV and average intergluon momentum $|\Delta \mathbf{p}_\perp|$ around 0.36 GeV, and $|\Delta x_i| \sim \frac{1}{3.5N}$, where N is the total number of particles.

Such a complicated object for large N has a very large enthropy and can be stable enough with respect to emission and reabsorption of quarks and gluons, and hence can be a prototype of the structures of the ridge type, observed in pp and AA collisions [65, 66], [67].

We have also shown, that the appearance of a multihybrid at some stage of the evolution does not violate the observed pdf's of gluons, valence quarks and sea quarks, however at very large $E^2 \sim Q^2/x$ one possibly needs combined effects of both reggeons and multihybrids.

Moreover, an ensemble of multihybrids yielding a balance of perturbative and np features different from the standard approach [68, 69], can be a reasonable alternative saturation state of the system evolution (see [70] for a discussion), since for a given excitation energy E of the system the set of equations for Fock components, leads to the effective cut-off of the number N of constituents, $N \approx \frac{E}{\varepsilon_g} \approx \frac{E}{0.8\ \mathrm{GeV}}$ and this set is subsequently hadronized. Finally, one should stress some similarity between the multihybrid mechanism and the Lund string model [71]. We note also, that the decay of a multihybrid can proceed or via gluon decay $g \to q\bar{q}$, or else via np decay of the string piece into $q\bar{q}$, which initiate different genealogical chains. Note also, that the strong np decay into $q\bar{q}$ pair can be accompanied by pion emission, – the phenomenon observed e.g. in the heavy quarkonia [72, 73, 74], which can produce pions at the earliest stages of evolution.

The author is grateful for useful discussions to K.G.Boreskov, B.L.Ioffe, O.V.Kancheli and members of the ITEP theory seminar and to I.M.Dremin and members of the FIAN theory seminar. The author gratefully acknowledges the help of I.V.Musatov in working out the material of appendix 2. The financial support of the RFBR grant 1402-00395 is gratefully acknowledged.

Appendix 1

Calculation of the $q\bar{q}g$ Green's function in the path integral formalism

We start with the path integral form of the free Green's function

$$g(x,y)=\left(\frac{1}{m^2-D^2}\right)_{xy}=\sqrt{\frac{T}{8\pi}}\int_0^\infty\frac{d\omega}{\omega^{3/2}}(D^2z)_{\mathbf{xy}}e^{-K(\omega)}=\sqrt{\frac{T}{8\pi}}\int\frac{d\omega}{\omega^{3/2}}\langle\mathbf{x}|e^{-H(\omega)T}|\mathbf{y}\rangle \tag{A1.1}$$

where $T=x_4-y_4$ and

$$K(\omega)=\int_0^T dt_E\left(\frac{\omega}{2}+\frac{m^2}{2\omega}+\frac{\omega}{2}\left(\frac{d\mathbf{z}}{dt_E}\right)^2\right),\quad H(\omega)=\frac{\mathbf{p}^2+m^2}{2\omega}+\frac{\omega}{2}. \tag{A1.2}$$

In a similar way for the product of two spinor $q,\bar{q}$ Green's function one has

$$G_{q\bar{q}}(x,y)=\left(\frac{(m_1-\hat{D}_1)(m_2-\hat{D}_2)}{(m_1^2-\hat{D}_1^2)(m_2^2-\hat{D}_2^2)}\right)_{xy}=\frac{T}{8\pi}\int_0^\infty\frac{d\omega_1}{\omega_1^{3/2}}\int_0^\infty\frac{d\omega_2}{\omega_2^{3/2}}\times$$

$$\times(D^3z_1)_{\mathbf{xy}}(D^3z_2)_{\mathbf{xy}}e^{-K_1(\omega_1)-K_2(\omega_2)}\langle YW\rangle \tag{A1.3}$$

where

$$4Y=tr\ \Gamma(m_1-\hat{D}_1)\Gamma(m_2-\hat{D}_2);\quad W=tr\exp ig\int_C A_\mu dz_\mu \tag{A1.4}$$

and we have omitted for simplicity the spin-dependent terms in W. To implement the gluon lines in the total amplitude, we can write the path-integral form

$$\langle A_\mu(u)A_\nu(v)\rangle=\delta_{\mu\nu}\int dse^{-K}(D^4z)_{uv}\Phi(u,v) \tag{A1.5}$$

where $\Phi(u,v)=P\exp(ig\int_v^u A_\lambda dz_\lambda)$.

We also take into account the identities [14, 15, 16, 17, 18, 19, 20], last reference,

$$(D^4z)_{xy}=(D^4z)_{xu}d^4u(D^4z)_{uy} \tag{A1.6}$$

$$\int_0^\infty ds\int_0^s d\tau_1\int_0^{\tau_1}d\tau_2 f(s,\tau_1,\tau_2)=\int_0^\infty ds\int_0^\infty d\tau_1\int_0^\infty d\tau_2 f(s+\tau_1+\tau_2,\tau_1+\tau_2,\tau_2). \tag{A1.7}$$

Our purpose is to write the path integral representation of the diagram in Fig.1. Using (A1.3), (A1.6) and (A1.7) one can write

$$G_{q\bar{q}}(x,y)=\int ds_1 d\tau_1 da_1 ds_2 d\tau_2 da_2 (D^4z)_{xu} d^3u 2\omega_{12}(D^4z)_{uv} d^3v 2\omega_{23}\times$$

$$\times(D^4z)_{vy}\hat{T}W_\sigma e^{-K_1-K_2}(D^4z')_{xu'}d^3u'2\omega'_{12}(D^4z')_{u'v'}d^3v'2\omega'_{23}(D^4z)_{v'y}\int ds'\, e^{-K_g}(D^4z)_{uv}W_A. \tag{A1.8}$$

One can now use the correspondence in (A1.1) to introduce the Hamiltonians H_1, H_2, H_3 for three sectors 1,2,3 shown in Fig.1, namely

$$\int ds_1 (D^4z)_{xu} e^{-K_1} = \sqrt{\frac{t}{8\pi}}\int \frac{d\omega_1}{\omega_1^{3/2}}\langle \mathbf{x}|e^{-H_1 t}|\mathbf{u}\rangle \tag{A1.9}$$

and similarly for H_2, H_3. As a result the total $q\bar{q}$ Green's function after integrating out the c.m. coordinates is

$$G_{\mathbf{p}}(T)=\int G_{q\bar{q}}(x,y)e^{i\mathbf{p}(\mathbf{x}-\mathbf{y})}d^3(\mathbf{x}-\mathbf{y})=$$

$$=\frac{\langle Y\rangle}{4}\int\frac{t}{2\pi}\frac{d\omega_1 d\omega_2}{(\omega_1\omega_2)^{3/2}}\langle 0|e^{-H_1 t}|\boldsymbol{\rho}_u\rangle d^3\boldsymbol{\rho}_u 2\omega_{12}2\omega'_{12}\frac{t'-t}{8\pi}\frac{d\omega'_1 d\omega'_2}{(\omega'_1\omega'_2)^{3/2}}\times$$

$$\times\sqrt{\frac{t'-t}{8\pi}}\frac{d\omega'_3}{\omega_3'^{3/2}}\langle\boldsymbol{\rho}_u,\boldsymbol{\rho}'_u\; e^{-H_2(t'-t)}|\boldsymbol{\rho}_v,\boldsymbol{\rho}'_v\rangle d^3\boldsymbol{\rho}_v 2\omega_{23}2\omega'_{23}\times$$

$$\times\frac{T-t'}{8\pi}\int\frac{d\omega''_1 d\omega''_2}{(\omega''_1\omega''_2)^{3/2}}\langle\boldsymbol{\rho}_v|e^{-H_3(T-t')}|0\rangle dt dt' \tag{A1.10}$$

and finally, integrating over Euclidean time intervals, one obtains

$$G_{q\bar{q}}(E)=\int G_{\mathbf{p}}(T)e^{iET}dT=\frac{\langle Y\rangle}{(2\omega)^2}\varphi_1(0)\frac{1}{E-E_1}\frac{V_{12}}{\sqrt{2\omega_g}}\frac{1}{E-E_2}\frac{V_{23}}{\sqrt{2\omega_g}}\frac{1}{E-E_3}\varphi_2(0) \tag{A1.11}$$

where V_{ik} are defined as (see also [32])

$$V_{ik}\equiv V_{ik}^{(\mu)}=g\int\varphi_M(\mathbf{r})\;{}^{\mu}\psi_n^{+}(0,r)d^3r, \tag{A1.12}$$

where $\varphi_\mu^{(k)}(\mathbf{r})$ and ${}^{\mu}\psi_n(\mathbf{r}_{12},\mathbf{r}_{23})$ are wave functions of the meson in the sector 1 or 3, and respectively of the hybrid with μ – the gluon spin orientation.

The form (A1.11) is exactly what is expected in the Fock component formalism of section 2.

Appendix 2

Integral representation for the 3 and 4 point functions

In this Appendix we shall consider the path integral technic [21, 22] for 3 and 4-point amplitudes with one closed quark contour and any number of perturbative and nonperturbative gluon interactions. The basic technic was described in [21, 22], and we start with the Euclidean space-time. Then the n-point amplitude defined as

$$G(p_i^{(1)}, ...p_n^{(n)}) = \langle J_1(p_1)...J_n(p_n)\rangle, \quad J_i(x) = \bar\psi(x)\Gamma_i\psi(x) \tag{A2.1}$$

can be written using [21] as

$$G(p_n^{(1)}...p_k^{(n)}) = \langle tr\prod_{i=1}^n \Gamma_i(m_i - \hat D_i)\int_0^\infty ds_i (Dz^{(i)})_{x^{(i)},x^{(i-1)}} e^{-K_i}\Phi_\sigma^{(i)} e^{ip^{(i)}x^{(i)}} dx^{(i)}\rangle. \tag{A2.2}$$

Here we have denoted

$$\Phi_\sigma^{(i)}(x^{(i)}, x^{(i-1)}) = P_A P_F \exp(ig\int_{x^{(i-1)}}^{x^{(i)}} A_\mu dz_\mu)\exp(g\int_0^{s_i} d\tau_i \sigma_{\mu\nu}F_{\mu\nu}), \tag{A2.3}$$

$$\sigma_{\mu\nu} \equiv \frac{1}{4i}(\gamma_\mu\gamma_\nu - \gamma_\nu\gamma_\mu),$$

and

$$(Dz^{(i)})_{xy} = \lim_{N\to\infty}\prod_{k=1}^N \frac{d^4\xi^{(i)}(k)}{(4\pi\varepsilon)^2}\frac{d^4q^{(i)}}{(2\pi)^4} e^{iq^{(i)}(\sum_k \xi^{(i)}(k) - (x-y))}, \quad N\varepsilon = s. \tag{A2.4}$$

Eq.(A2.2) is the exact expression in QCD, when no internal quark loops are present, so it should be exact in the large N_c limit.

All phase factors (A2.3) combine in (A2.2) into a Wilson loop factor with insertion of operators σF, which we denote as $\langle W_\sigma\rangle$,

$$\langle W_\sigma\rangle = \langle\prod_{i=1}^n \Phi_\sigma^{(i)}\rangle_A. \tag{A2.5}$$

In what follows we disregard the spin factors σF, in the first approximation since as it was shown in [14, 15, 16, 17, 18, 19, 20], they give nondominant contribution to the amplitude at large momenta. Moreover the $(m_i - \hat D_i)$ factors when acting on path integrals in (A2.2) are shown to be written as $(m_i - i\hat q_i)$, where q_i are Minkowskian momenta on the given line (see last reference in [14, 15, 16, 17, 18, 19, 20] for a derivation).

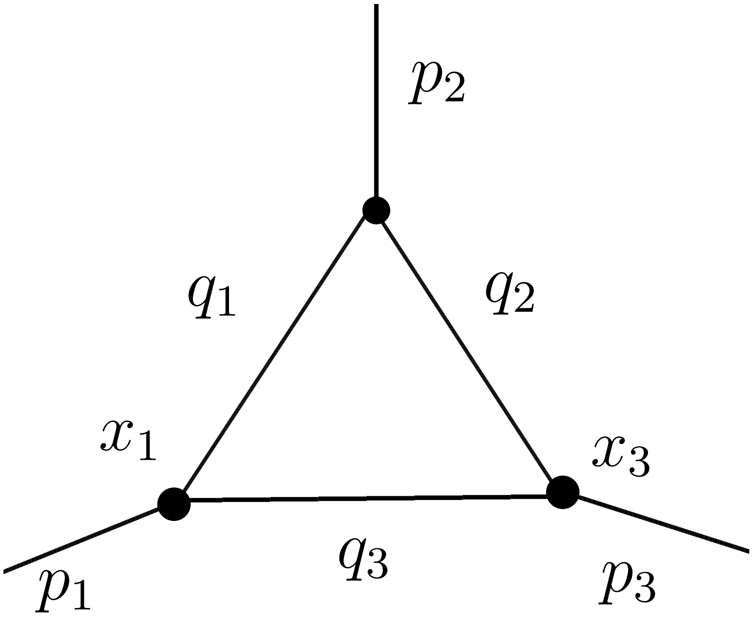

Figure 4:

We start here to calculate $\langle W_\sigma \rangle$ for the triangle diagram of Fig.5, making the approximation of large area, $S_{min} \gg T_g^2$, so that

$$\langle \langle W_\sigma \rangle_A \approx \exp(-\sigma S_{min}) \tag{A2.6}$$

Here $S_{min} = S_{min}(x^{(1)}, x^{(2)}, x^{(3)})$ and we assume for simplicity the straight-line (eikonal) geometry for the quark lines, so that the Nambu-Goto expression for S_{min} can written as

$$S_{min} = \int_0^1 dt \int_0^1 d\beta \sqrt{\dot{w}^2 (w')^2 - (\dot{w} w')^2}, \quad \dot{w} \equiv \frac{\partial w}{\partial t}, w' \equiv \frac{\partial w}{\partial \beta} \tag{A2.7}$$

and quark trajectories $\bar{z}_\mu$ (from $x^{(1)}$ to $x^{(3)}$) and z_μ (from $x^{(1)}$ to $x^{(2)}$) are given as

$$\begin{aligned} z_\mu(t) &= x_\mu^{(1)} + (x^{(2)} - x^{(1)})_\mu t \\ \bar{z}_\mu(t) &= x_\mu^{(1)} + (x^{(3)} - x^{(1)})_\mu t \end{aligned} \tag{A2.8}$$

with

$$w_\mu(\beta, t) = z_\mu(t)\beta + \bar{z}_\mu(t)(1-\beta). \tag{A2.9}$$

Since the Nambu-Goto form (A2.7) is difficult to handle, one introduces as usual einbein variables $\nu(\beta, t)$ and $\eta(\beta, t)$ to write

$$e^{-\sigma S_{min}} = \int D\nu D\eta e^{-2\int \nu[\dot{w}^2 + (\frac{\sigma}{\nu})^2 w'^2 - 2\eta(\dot{w}w') + \eta^2(w')^2] d\beta dt}. \tag{A2.10}$$

The form in the exponent in (A2.10) is quadratic in coordinates $x^{(i)}$ and can be easily computed to be

$$e^{-\sigma S_{min}} = \int D\bar{\nu} D\eta \exp\{-\sigma \frac{\bar{\nu}}{4} f\}, \tag{A2.11}$$

where

$$f \equiv y_1^2 + \frac{1}{\bar{\nu}^2} y_2^2 - 2\eta y_1 y_2 + \eta^2 y_2^2, \tag{A2.12}$$

and we have used notation $\bar{\nu} = \nu/\sigma$ and

$$y_1 \equiv x_{12} = x^{(1)} - x^{(2)}; y_2 \equiv x_{13} = x^{(1)} - x^{(3)}. \tag{A2.13}$$

The full integral over $x^{(i)}$ which is contained in (A2.2) can be written as

$$I_3 \equiv \int dx^{(2)} e^{i(p^{(1)}+p^{(2)}+p^{(3)})x^{(2)}} dy_1 dy_2 e^{i(p^{(1)}+p^{(3)})y_1 - ip^{(3)} y_2} \times$$

$$\times\, e^{iq_1 y_1 + iq_2(y_2 - y_1) - iq_3 y_2} \exp\{-\sigma \frac{\bar{\nu}}{4} f\} d\nu d\eta. \tag{A2.14}$$

The coordinate part of the integration in (A2.14) can be written as

$$J_3(a, b) \equiv \int d^4 y_1 d^4 y_2 e^{-(a_{ik} y_i y_k + b_i y_i)} = \left(\frac{\pi}{\det a}\right)^2 e^{-\frac{1}{4\sigma} b_i (a_{ik})^{-1} b_k} \tag{A2.15}$$

where notations are used

$$a_{11} = \frac{\bar{\nu}}{4}; \quad b_1 = -(p^{(1)} + p^{(3)}) - q_1 + q_2$$

$$a_{22} = \frac{1}{4}(\frac{1}{\bar{\nu}} + \eta^2 \bar{\nu}); \quad b_2 = p^{(3)} - q_2 + q_3$$

$$a_{12} = a_{21} = -\frac{\eta\bar{\nu}}{4}. \tag{A2.16}$$

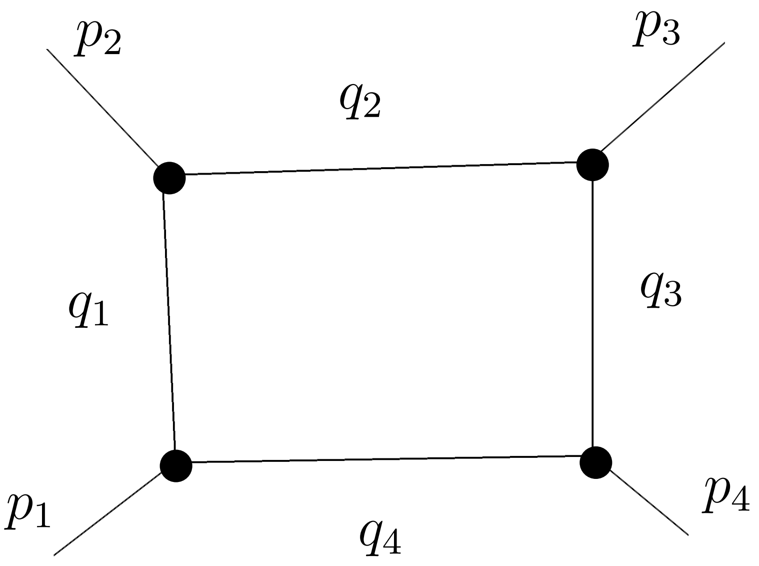

Figure 5:

Inserting (A2.15) into (A2.14) one has

$$I_3 = (2\pi)^4 \delta(\sum p^{(i)}) \int D\bar{\nu} \int D\eta \left(\frac{\pi}{\det a}\right)^2 \exp\left(-\frac{1}{4\sigma} b_i a_{ik}^{-1} b_k\right). \qquad \text{(A2.17)}$$

Since ν, η are nondynamical variables, the integrals over them can be taken using the stationary point analysis, which amounts to solving equations

$$\frac{\delta \Psi_3}{\delta \eta} |_{\eta=\eta_0} = 0, \quad \frac{\delta \Psi_3}{\delta \bar{\nu}} |_{\bar{\nu}=\nu_0} = 0, \qquad \text{(A2.18)}$$

with

$$\Psi_3 = -2 \ln \det a + \frac{1}{4\sigma} b_i a_{ik}^{-1} b_k. \qquad \text{(A2.19)}$$

Inserting $\bar{\nu} = \nu_0(p^{(i)}, q_i),\ \eta = \eta_0(p^{(i)}, q_i)$ back into (A2.17) one has $I_3^{(0)}(p^{(i)}, q_i)$ and the 3-point amplitude acquires the form

$$G(p^{(1)}, p^{(2)}, p^{(3)} = tr \prod_{i=1}^{3} \int d^4 q_i \Gamma_i (m_i - i\hat{q}_i) \int_0^\infty ds_1 e^{-s_i(m_1^2 + q_i^2)} I_3^{(0)}(p^{(i)}, q_i), \qquad \text{(A2.20)}$$

$$I_3^{(0)} = (2\pi)^4 \delta(\sum p^{(i)}) (16\pi)^2 \exp(-\frac{2}{\sigma} \sqrt{b_1^2 b_2^2 - (b_1 b_2)^2}). \qquad \text{(A2.21)}$$

The exponential factor in $I_3^{(0)}$ displays the role of confinement on the 3-point Green's function. Note first of all, that b_1, b_2 defined in (A2.16) and $b_3 = p^{(1)} + q_1 - q_3$ satisfy the relation $b_1 + b_2 + b_3 = 0$ and therefore one can check that the factor in the exponent in (A2.20) is symmetric with respect to the replacements $b_1, b_2 \to b_1, b_3 \to b_2, b_3$;

$$\tilde{S}(b_1, b_2) \equiv \sqrt{b_1^2 b_2^2 - (b_1 b_2)^2} = \tilde{S}(b_1, b_3) = \tilde{S}(b_2, b_3). \qquad \text{(A2.22)}$$

Secondly, the magnitude of b_i is the measure of "the off-shellness" in the corresponding vertex.

In the absence of confinement $J_3(a, b)$, Eq.(A2.15) goes over into the momentum conservation at each vertex,

$$J_3(a, b)|_{\sigma \to 0} = (2\pi)^8 \delta^{(4)}(b_1) \delta^{(4)}(b_2). \qquad \text{(A2.23)}$$

For nonzero σ the role of a smeared δ-functions is played by the exponential factor in (A2.21). It is clear that for large $p^{(i)}, (p^{(i)})^2 \gg \sigma$, this factor strongly cuts off all configurations of momenta unless $b_i^2 \lesssim \sigma, i = 1, 2$. This means that in the presence of confinement the momentum conservation at each vertex is fulfilled only with the absolute accuracy of the order of σ, i.e. $q_i - q_j = p^{(i)} + 0(\sqrt{\sigma})$.

As a result the Feynman rules for the triangle graph with the area law change in such a way that instead of one momentum integration inside the loop one has to do all three integrations over virtual momenta $q_i, i = 1, 2, 3$ with the cut-off factor (A2.21). This fact strongly changes the IR properties, since IR divergencies are now impossible by a simple power counting.

On the other hand, for large momenta, $(p^{(i)})^2 \gg \sigma$, $q_i^2 \gg \sigma$ the exponential factor in (A2.21) strongly cuts off the diagram magnitude unless only one momentum direction is available, while the perpendicular directions are controlled by σ. Consider now the 4-point function. According to the Fig.5, we assign the quark and antiquark trajectories as follows:

$$z_\mu(t) = x_{2\mu} + (x_3 - x_2)_\mu t$$

$$\bar{z}_\mu(t) = x_{1\mu} + (x_4 - x_1)_\mu t; \quad 0 \leq t \leq 1 \qquad \text{(A2.24)}$$

and for the standard Nambu-Goto expression (A2.7) we define the straight-line metric paths w_μ:

$$w_\mu(\beta, t) = z_\mu(t)\beta + \bar{z}_\mu(t)(1 - \beta) \qquad \text{(A2.25)}$$

we also denote three independent distances:

$$y_1 = x_{12} = x_1 - x_2; \quad y_2 = x_{23} \equiv x_2 - x_3; \quad y_3 = x_3 - x_4, \quad y_4 = x_{41} = x_4 - x_1; \tag{A2.26}$$

with relation for y_i:

$$\sum_{i=1}^{4} y_i = 0. \tag{A2.27}$$

Using (A2.10) we define the same integral as in (A2.14) and the integral equivalent to (A2.15) appears to be:

$$J_4(a,b) = \int d^4y_1 d^4y_2 d^4y_4 \exp\{-[a_{ik}y_iy_k + b_iy_i]\}. \tag{A2.28}$$

It is convenient to extract string tension from a_{ik}, and define:

$$\nu = \sigma v, \quad a_{ik} = \sigma \bar{a}_{ik} \tag{A2.29}$$

where

$$\begin{gathered}
\bar{a}_{11} = \frac{1}{2}(\frac{1}{v} + \eta^2 v); \bar{a}_{22} = \frac{v}{6} + \frac{1}{6}(\frac{1}{v} + \eta^2 v) - \frac{\eta v}{4}; \\
\bar{a}_{44} = \frac{v}{6} + \frac{1}{6}(\frac{1}{v} + \eta^2 v) - \frac{\eta v}{4}; \bar{a}_{12} = \frac{1}{4}(\frac{1}{v} + \eta^2 v - \eta v); \\
\bar{a}_{14} = \frac{1}{4}(\frac{1}{v} + \eta^2 v - \eta v); \bar{a}_{24} = \frac{v}{12} + \frac{1}{6}(\frac{1}{v} + \eta^2 v); \\
\bar{a}_{ik} = \bar{a}_{ki}; \quad b_1 = -q_1 - q_3 - p_1 - p_4; \\
b_2 = q_2 - q_3 + p_3; \quad b_4 = q_3 - q_4 + p_4.
\end{gathered} \tag{A2.30}$$

The integral J_4 in(A2.28) is Gaussian and the result is

$$J_4(a,b) = \frac{\pi^2}{(\det a)^2} e^{\frac{1}{4} b_i (a_{ik})^{-1} b_k}. \tag{A2.31}$$

In this case as also for the 3-point function, both η and ν are to be found from equations equivalent to (A2.18), (A2.19).

One can simplify the foregoing expressions using the approximation, when the area of the (generally speaking) nonplanar quadrangle is replaced by the sum of areas of two triangles formed by 4 sides and one diagonal inside the quadrangle. This approximation is exact for the planar quadrangle and gives a larger area for a nonplanar case. It can be used to obtain a qualitative estimate and the upper bound for the area law correction to the 4-point amplitude.

With the notations from (A2.26) one can thus write for the area of the quadrangle,

$$S^{(4)}_{min}(1,2,3,4) \approx S^{(3)}_{min}(1,2,3) + S^{(3)}_{min}(1,3,4) = \frac{1}{2}\sqrt{y_1^2y_2^2-(y_1y_2)^2} + \frac{1}{2}\sqrt{y_3^2y_4^2-(y_3y_4)^2}. \tag{A2.32}$$

The equivalent of Eq.(A2.14) reads

$$I_4 \equiv (2\pi)^4\delta(\Sigma p^{(i)})\prod_{i=1}^{4} d^4y_i\frac{d^4\mathcal{P}}{(2\pi)^4}e^{ib_iy_i-\sigma S^{(4)}_{min}} \tag{A2.33}$$

with

$$b_1 = q_1 - p_2 - p_3 + \mathcal{P},\quad b_2 = q_2 - p_3 + \mathcal{P}, \quad b_3 = q_3 + \mathcal{P},\quad b_4 = q_4 + p_4 + \mathcal{P}. \tag{A2.34}$$

Using (A2.32) one obtains

$$I_4 = (2\pi)^4\delta(\Sigma p^{(i)})\int\frac{d^4\mathcal{P}}{(2\pi)^4}\left(\frac{4\pi}{\sigma}\right)^8 e^{-\frac{2}{\sigma}\sqrt{b_1^2b_2^2-(b_1b_2)^2}-\frac{2}{\sigma}\sqrt{b_3^2b_4^2-(b_3b_4)^2}} \equiv (2\pi)^4\delta(\Sigma p^{(i)})I_4^{(0)}. \tag{A2.35}$$

The final expression for the 4-point function $\bar{G}_4(p_1,p_2,p_3,p_4)$ (where the factor $(2\pi)^4\delta(\sum p_i)$ is separated out)

$$\bar{G}_4(p_i) = tr\prod_{i=1}^{4}\int d^4q_i\Gamma_i(m_i - i\hat{q}_i)\int_0^\infty e^{-s_i(m_1^2+q_1^2)}ds_iI_4^{(0)}(a,b)\exp(-\mathcal{Q}). \tag{A2.36}$$

The factor $\exp(-\mathcal{Q})$ in (A2.36) is equal

$$\exp(-\mathcal{Q}) = \exp\left[-\frac{g^2C_2}{8\pi^2}\sum_{i\le j}I_{i,j}(s_i,s_j,q_i,q_j)\right]. \tag{A2.37}$$

The vertex parts $I_{i,i+1}$ in (A2.37) may contain double logarithmic parts under the same conditions as for the 3-point function. One can see, that also in the 4-point case one arrives at the asymptotics at large $b_i^2 \gg \sigma$

$$J_4^{(0)}(a,b) \to \prod_{i=1,2,4}\delta^{(4)}(b_i). \tag{A2.38}$$

In this case the four d^4q_i integrations in (A2.36) reduce to a single one, as it should be for the standard Feynman diagram without confinement.

References

[1] R.P.Feynman, Photon-Hadron Interactions, W.A.Benjamin Inc. Reading MA, 1972.

[2] B.L.Ioffe, V.A.Khose, and L.N.Lipatov, Deep Inelastic Processes, North-Holland, 1984.

[3] B.L.Ioffe, V.S.Fadin and L.Lipatov, Quantum Chromodynamics, Cambridge University Press, Cambridge, U.K., (2010).

[4] F.J.Yndurain, The Theory of Quark and Gluon Interactions, 4th edition, Springer, 2006.

[5] M.E.Peskin and D.V.Schroeder, "Quantum Field Theory", Addison-Wesley Publishing Company, Reading 1995.

[6] K.A.Olive et al., (Particle Data Group), Chin. Phys. **C 38**, N9 (2014), p.122.

[7] S.Bethke, G.Dissertori and G.P.Salam, Quantum Chromodynamics, p.296.

[8] B.Foster, A.D.Martin and M.G.Vincter, Structure functions.

[9] V.N.Gribov and L.N.Lipatov, Sov. J. Nucl. Phys. **15**, 438 (1972).

[10] Yu.M.Dokshitzer, Sov. Phys. JETP **46**, 641 (1977).

[11] G.Altarelli and G. Parisi, Nucl. Phys. **B 126**, 298 (1977).

[12] G.Sterman, arXiv:1412.5698 [hep-ph].

[13] A.V.Efremov and A.V.Radyushkin, Mod. Phys. Lett.**A 24**, 2803 (2009); arXiv: 0911.1195 [hep-ph].

[14] H.G.Dosch, Phys. Lett. B **190**, 177 (1987).

[15] Yu.A.Simonov, Nucl. Phys. B **307**, 512 (1988).

[16] H.G.Dosch and Yu.A.Simonov, Phys. Lett. B **205**, 339 (1988).

[17] A.Di Giacomo, H.G.Dosch, V.I.Shevchenko, Yu.A.Simonov, Phys. Rept. **372**, 319 (2002).

[18] Yu.A.Simonov, Phys. At. Nucl. **67** 846 (2004).

[19] Yu.A.Simonov, Phys. At. Nucl. **67** 1027 (2004).

[20] Yu.A.Simonov and J.A.Tjon, Ann. Phys. (N.Y.) **300**, 54 (2002).

[21] Yu.A.Simonov, Phys. Rev. **D 88**, 025028 (2013).

[22] Yu.A.Simonov, Phys. Rev. **D 90**, 013013 (2014).

[23] Yu.A.Simonov, Phys. Rev. **D 88**, 053004 (2013).

[24] Yu.A.Simonov, Phys. Rev. **D 91**, 065001 (2015), arXiv: 1409.4964 [hep-ph].

[25] Yu.A.Simonov, arXiv: 1411.7223, v.4 [hep-ph].

[26] R.L.Jaffe and A.Manohar, Nucl. Phys. **B 337**, 509 (1990).

[27] X.Ji, Phys. Rev. Lett. **78**, 610 (1997), hep-ph/9603249.

[28] X.Ji, J.-H.Zhang and Y.Zhao, arXiv: 1409.6329.

[29] S.J.Brodsky, Nucl. Phys. Proc. Suppl. **90**, 3 (2000).

[30] S.J.Brodsky, H.C.Pauli and S.S.Pinsky, Phys. Rep. **301**, 299 (1998).

[31] Yu.A. Simonov, Phys. At. Nucl. **67**, 553 (2004); hep-ph/0306310.

[32] Yu.A. Simonov, Phys. At. Nucl. **64**, 1876 (2001); hep-ph/0110033.

[33] R. Jaffe and K. Johnson, Phys. Lett. **B 60**, 201 (1976).

[34] M. S. Chanowitz and S. R. Sharpe, Nucl. Phys. **B 222**, 211 (1983).

[35] T. Barnes, F. Close, and F. de Viron, Nucl. Phys. **B 224**, 241 (1983).

[36] N. Isgur and J. E. Paton, Phys. Rev. **D 31**, 2910 (1985).

[37] Yu.A. Simonov in: Proceeding of the Workshop on Physics and Detectors for DAΦNE, Frascati, 1991.

[38] Yu.A. Simonov, Nucl. Phys. B (Proc. Suppl.) **23 B**, 283 (1991),

[39] Yu.A. Simonov in: Hadron-93 ed. T. Bressani, A. Felicielo, G. Preparata, P.G. Ratcliffe, Nuovo Cim. **107 A**, 2629 (1994).

[40] Yu.S. Kalashnikova, Yu.B. Yufryakov, Phys. Lett.**B 359**, 175 (1995).

[41] Yu. Yufryakov, hep-ph/9510358.

[42] Yu.S.Kalashnikova and D.S.Kuzmenko, Phys. At. Nucl. **67**, 538 (2004); hep-ph/0302070.

[43] Yu.S.Kalashnikova and A.V.Nefediev, Phys.Rev. **D 77**, 0540025 (2008).

[44] S. Ishida, H. Sawazaki, M. Oda, and K. Yamada, Phys. Rev. **D 47**, 179 (1993).

[45] T. Barnes, F. Close, and E. Swanson, Phys. Rev. **D 52**, 5242 (1995).

[46] I. J. General, S. R. Cotanch, and F. J. Llanes-Estrada, Eur.Phys.J. **C 51**, 347 (2007).

[47] I. Balitsky, D. Diakonov, and A. Yung, Z. Phys. **C 33**, 265 (1986).

[48] J. Latorre, P. Pascual, and S. Narison, Z. Phys. **C 34**, 347 (1987).

[49] K. G. Chetyrkin and S. Narison, Phys. Lett. **B 485**, 145 (2000).

[50] S. Narison, Phys. Lett.**B 675**, 319 (2009).

[51] V.Mathieu, Phys. Rev. **D 80**, 014016 (2009).

[52] L.S.Kisslinger, Phys. Rev. **D 79**, 114026 (2009).

[53] C.Semay, F.Buisseret and D.Silvester-Brac, Phys. Rev. **D 79**, 094020 (2009).

[54] P.Guo et al., Phys. Rev. **D 77**, 056005 (2008).

[55] J.J.Dudek, Phys. Rev. **D 84**, 074023 (2011).

[56] B.Ketzer, arXiv: 1208.5125.

[57] S.Godfry and N.Isgur, Phys. Rev. **D 32** , 189 (1985).

[58] F.Bloch and A.Nordsick, Phys. Rev. **52**, 54 (1937).

[59] S. Weinberg, Phys. Rev. **140**, B 516 (1965).

[60] D.Yennie, S.Frautschi and H.Suura, Ann. Phys. **13**, 379 (1961).

[61] A.Le Yaouanc, L.Oliver, O.Péne etal., Z. Phys. **C 28**, 309 (1985).

[62] F.Iddir, S.Safir and O.Péne, Phys. Lett. **B 433**, 125 (1998).

[63] A.Yu.Dubin, A.B.Kaidalov and Yu.A.Simonov, Phys. At. Nucl., **58**, 300 (1995), hep-ph/9408212.

[64] V.P.Morgunov, V.I.Shevchenko and Yu.A.Simonov, Phys. lett. **B 416**, 433 (1998).

[65] CMS Collaboration, JHEP 1009 (2010) 091 [arXiv: 1009.4122 [hep-ex].

[66] Wei Li, Mod. Phys. Lett. **A27**, 1230018 (2012), arXiv: 1206.0148 [nucl. ex].

[67] M.Yu. Azarkin, I.M.Dremin and A.V.Leonidov, Mod. Phys. Lett. **A 26**, 963 (2011).

[68] M.Yu. Azarkin, I.M.Dremin and M.Strikman, Phys. Lett. **B 735**, 244 (2014).

[69] L.Frankfurt , M.Strikman and C.Weiss, Phys. Rev. **D 83**, 054012 (2011).

[70] F.Gelis, E.Iancu, J.Jalilian-Marian, R.Venugopalan, Ann. Rev. Nucl. Part. Sci. **60**, 463 (2010); arXiv:1002.0333 [hep-ph].

[71] Bo Andersson, S.Mohanty and F.Söderberg, arXiv: hep-ph/0212122.

[72] Yu.A.Simonov and A.I.Veselov, Phys. Rev. **D 79**, 034024 (2009).

[73] I.V.Danilkin, V.D.Orlovsky and Yu.A.Simonov, Phys. Rev. **D 85**, 034012 (2012).

[74] A.M.Badalian, V.D.Orlovsky and Yu.A.Simonov, Phys. At. Nucl. **76**, 955 (2013).